American Mineralogist, Volume 78, pages 968–979, 1993

Crystal chemistry of Fe^{3+} and H^+ in mantle kaersutite: Implications for mantle metasomatism

M. Darby Dyar
Department of Geology and Astronomy, West Chester University, West Chester, Pennsylvania, 19383, U.S.A.
Stephen J. Mackwell
Department of Geosciences, The Pennsylvania State University, University Park, Pennsylvania 16802, U.S.A.
Anne V. McGuire
Department of Geosciences, University of Houston, Houston, Texas 77204, U.S.A.
Laura R. Cross, J. David Robertson
Department of Chemistry and Center for Applied Energy Research, University of Kentucky, Lexington, Kentucky 40506, U.S.A.

Abstract

Chemical and crystal chemical analyses have been performed on a suite of subcontinental, mantle-derived hornblende (kaersutite) samples. Mössbauer techniques have been utilized to investigate Fe valence and site occupancies, U extraction techniques have been used to determine bulk H contents, proton-induced γ-ray emission (PIGE) analysis was employed to measure F, and electron microprobe techniques coupled with the above measurements have been utilized to determine major-element contents of hornblende. Similar analyses were performed on a suite of metamorphic amphibole samples from Cosca et al. (1991). Comparison with their wet chemical results on Fe^{3+}/Fe^{2+} permitted determination of $C = 1.22$, the correction for differential recoil-free fraction effects, which was used to correct the mantle sample Mössbauer data. The results of the analyses for the kaersutite samples show a nearly 1:1 inverse relationship between the Fe^{3+} and H^+ contents. Although the range of Fe^{3+}/H^+ in the less oxidized kaersutite samples may be explained by partial H loss during entrainment and ascent, the nearly total dehydrogenation of the Fe^{3+}-rich megacrysts would require time scales significantly longer than what is expected for transport. Thus, it seems likely that these oxykaersutite samples grew in a more oxidized metasomatic fluid, where incorporation of H was not required for charge compensation. As megacrysts from the same location show wide variation in Fe^{3+} and H^+, it appears likely that significant variations in the oxidation state of the mantle metasomatic fluid occurred over relatively small temporal or spatial scales.

Introduction

A 1964 paper by Oxburgh was among the first to suggest that the Earth's upper mantle must contain the mineral amphibole in order to provide sufficient K and other alkalis to serve as a source region for alkali volcanism. Because the presence of amphibole implies a significant volatile component in the mantle, this suggestion and related work by Varne (1970) led to numerous studies on the influence of volatiles on the melting behavior of peridotite (e.g., Bailey, 1970, 1972) and on the effects and characteristics of metasomatism (e.g., Menzies, 1983; Dick et al., 1984). Field observations (Wilshire and Shervais, 1975; Harte et al., 1975; Stosch and Seck, 1980; Roden et al., 1984; Wilshire, 1987; Nielson et al., 1993) have led to a variety of models for mantle metasomatic processes. There is current debate over the mechanisms that produce the different styles of metasomatism. For example, it is not understood why some styles of metasomatism are characterized by the presence of amphibole, while others lack hydrous phases. Improved understanding of the role of volatile species in metasomatism and the crystal chemistry of the hydrous phases is needed.

Recent mineralogical studies by Dyar et al. (1989, 1992a, 1992b) among others including Wood, Virgo, and coworkers have focused attention on the presence of Fe^{3+} in both typical mantle phases (McGuire et al., 1989; Wood and Virgo, 1989; Dyar et al., 1989; Canil et al., 1990) and in metasomatized peridotites (McGuire et al., 1991; Dyar et al., 1992a). The studies on peridotite indicate that contrasting styles of metasomatism are associated with distinctive sets of Fe^{3+}/Fe_{tot} ratios in component phases; they are also suggestive of an interrelationship between Fe^{3+} and H^+ in individual minerals.

The goal of our present research is to examine the crystal chemistry of mantle-derived amphibole by studying its major-element contents, Fe-site occupancies and valences, and H^+ content and partitioning behavior. Data on the isotopic behavior of H are presented in brief in

0003–004X/93/0910–0968$02.00

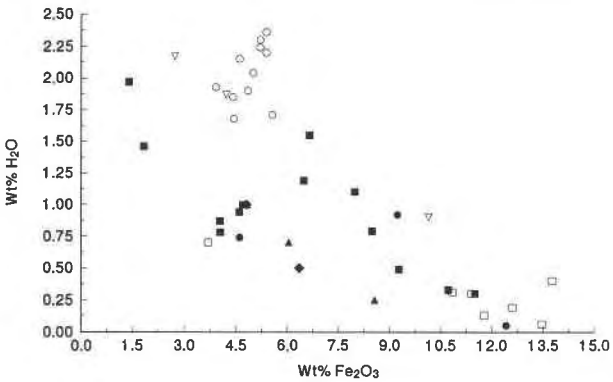

Fig. 1. Fe_2O_3 and H_2O contents of oxykaersutites and mantle amphiboles. Symbols represent data from Barnes (1930), solid circles; Aoki (1963), solid squares; Best (1970), solid triangles; Wilshire and Trask (1971), solid diamonds; Aoki (1971), open circles; Boettcher and O'Neil (1980), open squares; and Graham et al. (1984), open triangles. The lack of a closely aligned linear trend among these variables arises from three main factors: (1) H_2O was, in most cases, determined by weight loss with no discrimination of possible CO_2 contribution; (2) Fe_2O_3 was, in most cases, determined by calorimetry, which could not detect contributions from Ti and Mn oxidation; and (3) since the true substitution here involves oxidation of Fe^{2+} to Fe^{3+} due to loss of H^+ ions, the plot of oxide data obscures any evidence of a crystal chemical trend.

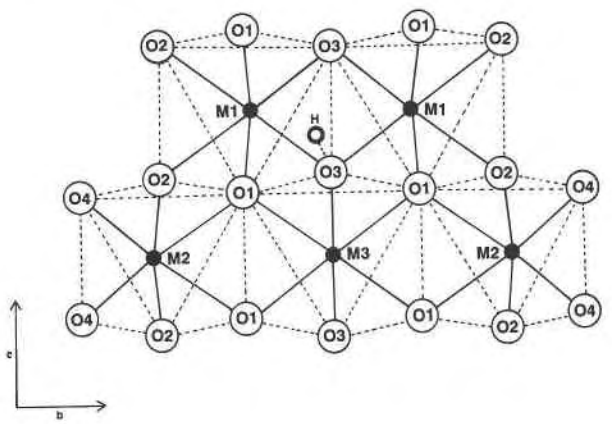

Fig. 2. Schematic drawing of the octahedral sites adjacent to the H^+ atoms in the hornblende structure. O sites are indicated by large outlined circles and identified by their numbers; cation sites are small, solid circles. The H atom sits close to the O3 site with an O-H distance of 0.934 Å (Pechar et al., 1989), and so the OH group takes part in the coordination polyhedra of both M1 and M3.

Dyar et al. (1992b) and will be pursued, together with O isotope data, in a later work (Dyar et al., in preparation). We present here the results of a detailed study of 20 kaersutite samples, in order to assess the relationships among H^+, Fe^{3+}, and other major elements within the amphibole structure.

Background

Beginning with Barnes (1930) and then Winchell (1945), Aoki (1963, 1970; 1971), Best (1970, 1974), and Ernst and Wai (1970), geochemists have used atomic absorption and wet chemical analyses to study the dehydration of amphibole. Incomplete characterization of minor constituents such as Cr^{3+} and Ti^{4+} and suspicions that Ti^{3+} might contribute to errors in Fe^{3+} determinations hampered these workers in evaluating the detailed crystal chemistry of their samples. Furthermore, H_2O analyses were generally determined by weight loss, a technique that yielded results greatly biased by the contents of other volatile phases, especially CO_2, which are now known from fluid inclusion studies to be abundant in minerals derived from the upper mantle (see e.g., Roedder, 1965; Bergman, 1981; Andersen et al., 1984).

More recent geochemical and petrologic studies of amphibole have focused more closely on major-element analyses coupled with studies of H isotope behavior. Kuroda et al. (1978) examined δD of hornblende from intrusions in alkali basalts; Boettcher and O'Neil (1980) followed with a thorough examination of δD, H_2O content, and $\delta^{18}O$ in amphibole; and Graham et al. (1984) derived activation energies for H isotope exchange. Matson et al. (1984) examined the major-element and volatile components of amphibole in xenoliths from the Grand Canyon and found a strong positive correlation between Ti contents and H^+ deficiency. An intriguing study (Bryndzia et al., 1990) investigated the relationship among f_{O_2}, OH^- content, δD, and Fe^{3+}/Fe_{tot} in samples from Sheppard and Epstein (1970) and Kuroda et al. (1978) and found only small ranges of δD and Fe^{3+}/Fe_{tot}; however, no primary data were given. Recent work by Deloule and coworkers (e.g., Deloule et al., 1990, 1991) has concentrated solely on the isotopic variation displayed by hornblende. Unfortunately, none of these more recent studies included complete (published) Fe^{3+} data on all samples, and so other workers (e.g., Boettcher and O'Neil, 1980) could do little more than note a general inverse correlation between Fe_2O_3/FeO and H_2O content (Fig. 1).

Many crystallographic studies of the kaersutite structure using X-ray diffraction have been published, including Papike and Clark (1968), Papike et al. (1969), Kitamura and Tokonami (1971), and Hawthorne and Grundy (1973). Powder (Jiràk et al., 1986) and single-crystal (Pechar et al., 1989) neutron diffraction studies of this mineral have further improved our understanding of the cation distributions and H positions in kaersutite (Table 1, Fig. 2).

Additional relevant X-ray data complemented by experimental work has been performed recently by Popp et al. (1990) at Texas A&M University (Phillips et al., 1988, 1989; Clowe et al., 1988). Results showed that dehydrogenation accompanying heat treatment causes preferential ordering of trivalent cations at the cis-M1 and trans-M3 sites. Some trivalent cations in M2 may relocate to M1 or M3 as oxidation occurs. Fe^{3+}-H^+ oxysubstitution and Al substitution were identified as the primary mechanisms accompanying oxidation and dehydrogenation. Popp et al. (1990) surveyed the literature on Fe^{3+}-rich

TABLE 1. Cation distributions in kaersutite based on structure refinements

Site	Hawthorne and Grundy (1973)	Pechar et al. (1989)	Phillips et al. (1989)
A	$Na_x + K_y$ and $Na_{0.543-x}$ and $K_{0.434-y}$*	0.265Na + 0.205K	0.43Na
T1	0.53Si + 0.47Al	0.57Si + 0.43Al	0.35Al + 0.65Si
T2	0.94Si + 0.06Al	0.90Si + 0.10Al	0.02Al + 0.98Si
M1	$0.343Fe^{3+}$ + 0.657Mg	0.26Ti + 0.03Ca + $0.32Fe^{3+}$ + 0.39Mg	0.415Fe + 0.585Mg
M2	$0.056Fe^{3+}$ + 0.502Mg + 0.185Al + 0.257Ti	0.17Al + $0.18Fe^{3+}$ + 0.65Mg	0.214Fe + 0.321Mg
M3	$0.235Fe^{3+}$ + 0.765Mg	0.93Mg + $0.01Fe^{2+}$ + $0.06Fe^{3+}$	0.588Fe + 0.412Mg
M4	0.009Mn + 0.958Ca + $0.010Fe^{3+}$ + 0.025Mg	0.99Ca + 0.01Mn	0.915Ca + 0.099Ca
H	—	0.51H	1.0H

* The variables x and y are related by the equation $x + 1.8y = 0.802$.

calcic and subcalcic amphibole and found that the relation between the Fe^{3+}-oxyamphibole component and the OH^- content of amphibole could not be quantified, although the lack of large numbers of high-quality amphibole analyses greatly limited their conclusions.

Numerous Mössbauer studies of amphibole samples exist in the literature, as summarized by Hawthorne (1983). As he noted, the interpretation of spectra of calcic amphibole minerals, in particular, is "not straightforward." Most of the controversy revolves around proper interpretation of the doublets resolved in the spectra relative to their assignment to the known crystallographic sites in the structure. In principle, four doublets corresponding to Fe^{2+} in each of the metal sites of the structure might be observed in a spectrum of Fe^{2+}-rich amphibole. Additional doublets corresponding to Fe^{3+} in those sites are also possible, although Fe^{3+} in the M4 site would be unlikely except in Ca or Na-deficient samples. Goodman and Wilson (1976), in fact, resolved five doublets in a single hornblende spectrum, which they assigned to Fe^{2+} in M1–M4 and to Fe^{3+}_{tot}. Other workers have observed smaller numbers of doublets (Burns et al., 1970; Burns and Greaves, 1971; Bancroft and Brown, 1975; Goldman and Rossman, 1977) on tremolite-ferroactinolite solutions. The question of Fe^{2+} occupancy in M4 remains controversial (e.g., Aldridge et al., 1982); it is apparent that Fe^{2+} will occupy the M4 site only in the rare cases where $Ca^{2+} + Na^+ + K^+$ is insufficient to fill the site. Occupancy of Fe^{3+} in M4 seems, therefore, extremely unlikely. One additional conclusion from these previous studies is germane to the discussion at hand: the distortions of the M sites in calcic amphibole, which are known to decrease in the order M4, most distorted, to M2 to M3 to M1, least distorted, can be related to the quadruple splittings observed for Fe^{2+} in the order M4, lowest quadruple splitting (Δ), to M2 to M3 to M1 (Hawthorne, 1981). No Mössbauer studies of Fe^{3+}-rich kaersutite samples could be found in the literature, with the exception of Schwartz and Irving (1978) and McGuire et al. (1989); both of these focused more on the amount of Fe^{3+} than on its distribution. However, on the basis of the increasing distortion and decreasing Δ relationship observed by Hawthorne (1978, 1981), it would be possible to predict relative quadrupole splittings of Fe^{3+} doublets if they could be resolved (i.e., in the spectrum of a Fe^{3+}-rich amphibole). As noted by Burns et al. (1985), although high Δ implies low distortion for Fe^{2+} in silicates, high Δ implies high distortion for Fe^{3+}. Therefore we would predict the highest Δ for Fe^{3+} in the M2 site (assuming no Fe^{3+} in M4) and gradually decreasing Δ for Fe^{3+} in the order M3 to M1, which can be used in site assignments for the observed doublets.

One final comment regarding the interpretation of Mössbauer spectra of amphibole is important within the context of the literature. It is well known that the area of a Mössbauer doublet (pair of peaks) is a function of peak width Γ, sample saturation $G(x)$, and the Mössbauer recoil-free fraction f. Bancroft (1973) used the following formulation for area ratios:

$$\frac{A_{Fe^{3+}}}{A_{Fe^{2+}}} = C\frac{N(Fe^{3+})}{N(Fe^{2+})}$$

where N is the amount of each species found by wet chemical analyses. It follows that C may be expressed as

$$C = \frac{\Gamma_{Fe^{3+}} + f_{Fe^{3+}} + G(x)_{Fe^{3+}}}{\Gamma_{Fe^{2+}} + f_{Fe^{2+}} + G(x)_{Fe^{2+}}}.$$

Bancroft and Brown (1975) determined that saturation corrections are unnecessary for samples mixed with sugar. The $\Gamma_{Fe^{2+}}$ and $\Gamma_{Fe^{3+}}$ were also determined to be equal by them. However, when the Mössbauer data on hornblende reported by Bancroft and Brown (1975) were compared with wet chemical Fe^{3+}/Fe^{2+} ratios determined by Dodge et al. (1968), a C value of 1.13 ± 0.02 was derived (on the basis of seven samples). A later study reported C values of 1.36, 1.25, and 1.24 for a hastingite and two kaersutite samples, respectively (Whipple, 1972).

More recently, four samples studied by Schwartz and Irving (1978) yielded Fe^{3+}/Fe^{2+} values that were higher when determined by chemical means than by Mössbauer spectroscopy (resulting in a C value of <1). They attributed the difference to the presence of Ti^{3+} in their samples. The only other comparison of chemical and Mössbauer Fe^{3+}/Fe^{2+} ratios was performed by Bahgat and Fayek (1982), who derived a C value of 1.15 based on one sample. One of the goals of this work was to constrain this relationship and determine a realistic value for C.

SAMPLE SELECTION, PREPARATION, AND ANALYSES

Hornblende megacrysts were selected for this study from the extensive collections of Howard Wilshire and Robert

Coleman of the U.S. Geological Survey. The Coleman collection has since been curated by the National Museum of Natural History, Smithsonian Institution. Source localities for all samples studied are listed in Table 2; all specimens came from basalt hosts erupted in continental rift environments. Small pieces for thin sections were removed from each megacryst. Additional pieces were broken off and ground by hand under acetone (to prevent oxidation) into fragments <1 mm to facilitate hand-picking of grains. Only pristine hornblende grains were used for this study; any grains containing visible alteration, inclusions, or impurities were rejected. Approximately 680 mg of separates were prepared: 150 mg for Mössbauer analyses, 100 mg for PIGE, 30 mg for O isotope study, and 400 mg for H^+ extraction. In addition, 300-mg aliquots of metamorphic amphibole samples (Cosca et al., 1991) were obtained from Michael Cosca for the comparative study of *C*.

Electron microprobe analyses were performed on the Jeol 733 electron microprobe at Southern Methodist University, using a Krisel automation package. Routine analytical conditions were used: 15-keV acceleration voltage, 20-nA beam current measured on a Faraday cup, 30-s count times, and the Bence-Albee correction routine supplied by Krisel. At least five points were analyzed on each megacryst, and only unzoned samples were used. Compositions for AK-M1, AK-M2, and H366A are described in McGuire et al. (1989); the analysis used for H366-92 was made using XRF techniques at Washington State University. Analytical errors are ±0.5–2% for major elements and ±10–20% for minor elements.

Mössbauer analyses were performed in the Mineral Spectroscopy Laboratory at the University of Oregon. A source of 50–20 mCi ^{57}Co in Pd was used on an Austin Science Associates constant acceleration spectrometer. Results were calibrated against an α-Fe foil of 6 μm thickness and 99% purity. Spectra were fitted using a version of the program Stone modified to run on IBM and compatible personal computers. The program uses a nonlinear regression procedure with a facility for constraining any set of parameters or linear combination of parameters. Lorentzian line shapes were used for resolving peaks, as there was no statistical justification for the addition of a Gaussian component to the peak shapes. Fitting procedures in general followed those described in Dyar et al. (1989) and McGuire et al. (1989). A statistical best fit was obtained for each model for each spectrum using the χ^2 and Misfit parameters; practical application of these parameters is discussed elsewhere (Dyar, 1984). Errors are estimated at ±3% for doublet areas and ±0.02 mm/s for peak width, isomer shift, and quadrupole splitting.

H contents were determined by means of a procedure for collecting and measuring all the structural H using a volumetric measurement of H_2O vapor extracted from silicates (see Bigeleisen et al., 1952; and Holdaway et al., 1986, for details of the technique). In general, clean mineral separates are degassed under vacuum for at least 8 h at 50–85 °C to evaporate adsorbed atmospheric moisture.

TABLE 2. Hornblende localities represented

DL-5	Deadman Lake, California, Hill 2237
DL-7	Deadman Lake, California, Hill 2237
DL-9	Deadman Lake, California, Hill 2284
AK-M1	Harrat al Kishb, Saudi Arabia, Coleman locality H271
AK-M2	Harrat al Kishb, Saudi Arabia, Coleman locality H271
AK-M3	Harrat al Kishb, Saudi Arabia, Coleman locality H271
AK-M4	Harrat al Kishb, Saudi Arabia, Coleman locality H271
AK-M5	Harrat al Kishb, Saudi Arabia, Coleman locality H274
Ba-5	Dish Hill, California
Tm	Easy Chair Crater, Lunar Crater, Nevada
Fr-11	Massif Central, France, just east of Alleyras basalt flow
Fr-12	Massif Central, France, Montgros, from oxidized vent agglomerate
84-BR	Dreiser Weiher, Germany, Brück-Raders cone, cognate
86-BM	Bullenmerri maar, Victoria, Australia
86-LEH*	Lake Eacham maar, Queensland, Australia
H366A	Harrat Hutaymah, Saudi Arabia
H366-92	Harrat Hutaymah, Saudi Arabia
S.C.	San Carlos, Arizona, USNM 111312.0023
K.N.Z.	Kakanui, New Zealand, USNM 109647/50
Eifel	Eifel Volcanic Field, USNM 114856.0006

Note: although the sample numbers listed here may resemble numbers given in previous studies, such as Boettcher and O'Neil (1980), they bear no relation to previously studied samples except for locality.

* Sample 86-LEH consists of amphibole grains, rather than a megacryst, separated from a spinel peridotite xenolith found at this locality.

Samples are then fused in an induction furnace to liberate structural H_2O. Distillation processes involving transfer of evolved gases through a series of traps employing liquid N_2 and a slush of methanol and dry ice are used to separate H_2O molecules effectively from other condensable and noncondensable gases. H_2O vapor is then passed over hot U (>750 °C) to liberate free H^+. A Hg-piston Toepler pump is used to collect vapor in a volumetrically calibrated reservoir for yield measurement. For this study, every fifth sample was analyzed twice; distilled H_2O was used for calibration. All data are corrected for a sample blank of 2.5 torr (roughly 0.5–2% of the total wt% H_2O, depending on sample size and volume of H_2O vapor). Errors are estimated at ≤0.1 wt% H_2O based on replications.

F concentrations were determined by external-beam proton-induced γ-ray emission analysis (PIGE) at the University of Kentucky Van de Graaff Accelerator Laboratory. The inelastic proton scattering reactions on ^{19}F at proton bombarding energies of 3.5 and 2.5 MeV were utilized. Details of the method are included in Wong et al. (1992). Minimum detection limits of 5 ppm with standard deviations of 20–140 ppm were obtained.

RESULTS

Mössbauer data

Interpretation of the Mössbauer data measured for this study proves extremely difficult because of the wide range of the Fe^{3+} contents of the samples (from 100 to 27% Fe^{3+}). Both Fe^{3+} and Fe^{2+} can occupy (in theory) any of the four M sites in the structure, although Fe^{3+} in M4 would be unlikely in this composition range. This would give rise to a total of eight possible doublets (realistically, seven) in each spectrum. In practice, it is impossible to resolve those doublets in a statistically meaningful fash-

TABLE 3. Mössbauer results for six peak fits

	Fe^{3+}				Fe^{2+}				Fe^{2+}						
Sample	I.S.	Q.S.	W	A	I.S.	Q.S.	W	A	I.S.	Q.S.	W	A	%Mis	%Un	χ^2
DL-5	0.38	0.78	0.54	38	1.13	2.56	0.33	29	1.12	2.05	0.41	32	0.06	0.01	621
DL-7	0.42	0.69	0.49	46	1.12	2.56	0.32	25	1.08	2.13	0.41	29	0.08	0.01	735
DL-9	0.39	1.40	0.51	43											
	0.40	0.85	0.43	56					1.06	2.38	0.30	1	0.03	0.01	561
AK-M1	0.38	0.74	0.49	32	1.13	2.52	0.33	30	1.12	2.01	0.40	38	0.04	0.01	591
AK-M2	0.38	0.75	0.49	29	1.13	2.51	0.34	33	1.13	1.99	0.38	38	0.00	0.00	507
AK-M3	0.38	0.73	0.50	32	1.13	2.51	0.35	33	1.12	2.00	0.39	35	0.12	0.01	812
AK-M4	0.38	0.71	0.54	33	1.13	2.48	0.35	35	1.12	1.96	0.37	32	0.13	0.01	812
AK-M5	0.38	0.74	0.54	41	1.14	2.54	0.30	23	1.12	2.02	0.40	36	0.19	0.02	819
Ba-5	0.38	0.81	0.55	40	1.12	2.57	0.37	30	1.12	2.04	0.41	30	0.01	0.01	531
Tm	0.41	0.94	0.57	80	1.03	2.70	0.27	4	1.12	2.06	0.38	16	−0.01	−0.01	531
Fr-11	0.41	0.90	0.57	76	1.07	2.59	0.34	12	1.10	2.05	0.34	12	0.01	0.00	532
Fr-12	0.38	1.56	0.44	23											
	0.40	1.16	0.46	53											
	0.40	0.70	0.34	24									0.00	0.00	515
84-BR	0.38	0.84	0.56	49	1.12	2.62	0.34	29	1.10	2.13	0.40	22	0.13	0.01	933
86-BM	0.37	0.76	0.55	27	1.13	2.56	0.33	33	1.13	2.04	0.43	40	0.03	0.01	566
86-LEH	0.40	0.75	0.53	31	1.13	2.56	0.35	32	1.13	1.99	0.42	37	0.09	0.01	677
H366A	0.39	0.79	0.45	28	1.14	2.59	0.30	32	1.15	2.08	0.45	44	0.06	0.01	585
H366-92	0.39	1.31	0.59	50											
	0.40	0.81	0.42	43	1.09	2.40	0.27	4	1.11	1.92	0.23	3	0.00	0.00	524
San Carlos	0.43	0.63	0.61	37	1.12	2.40	0.40	24	1.08	1.90	0.52	39	0.02	0.01	527
Kakanui	0.37	0.72	0.57	33	1.13	2.60	0.33	31	1.12	2.09	0.42	36	0.03	0.01	550
Eifel	0.37	0.73	0.55	46	1.12	2.56	0.31	24	1.11	2.05	0.40	30	0.02	0.01	525
Average	0.39	0.87	0.51	41.3	1.06	2.41	0.31	24.4	1.11	2.05	0.39	28.9			
S.D.	0.02	0.24	0.06	14.2	0.25	0.57	0.08	10.7	0.02	0.10	0.06	12.1			
SSA-5	0.35	0.79	0.35	33	1.13	2.70	0.28	33	1.16	2.18	0.43	34	0.01	0.01	525
HL862C	0.36	0.77	0.37	38	1.13	2.69	0.29	36	1.17	2.13	0.44	26	0.03	0.01	537
MR-865A	0.36	0.76	0.34	25	1.13	2.68	0.30	41	1.15	2.06	0.46	34	0.01	0.01	521
MIN 864	0.36	0.77	0.37	38	1.13	2.69	0.29	36	1.17	2.13	0.44	26	0.03	0.01	536
SSA-10	0.35	0.79	0.38	28	1.14	2.67	0.27	32	1.14	2.15	0.42	40	0.02	0.01	522
FA86-1	0.35	0.78	0.37	21	1.13	2.59	0.31	40	1.13	2.07	0.41	39	0.02	0.01	528
HL8611	0.34	0.81	0.36	36	1.13	2.70	0.26	29	1.17	2.20	0.40	35	0.01	0.01	520
SAS-13	0.37	0.76	0.41	38	1.13	2.62	0.30	34	1.13	2.09	0.40	28	0.04	0.02	546

Note: I.S. = isomer shift, in millimeters per second. Values given are ±0.02 mm/s (Dyar, 1984). Q.S. = quadrupole splitting, in millimeters per second. Values given are ±0.02 mm/s (Dyar, 1984). W = peak width, in millimeters per second. Values given are ±0.02 mm/s (Dyar, 1984). A = peak area, in percent of total area. Values given are ±2% of the total area (Dyar, 1984). Other abbreviations: %Mis = percent of Misfit (Ruby, 1973); %Un = percent of uncertainty of fit (Ruby, 1973); χ^2 = chi squared; S.D. = standard deviation. Mössbauer parameters are referenced to Fe metal foil calibration.

ion because of their heavily overlapping peak positions. As noted above, previous workers have resolved doublets assigned to as many as four Fe^{2+} sites and one Fe^{3+} site. Such assignments are difficult to determine in our mantle kaersutite suite because none of these hornblende samples has a stoichiometric amount of H^+. Some of the cations in the M1 and M3 sites will not have their expected geometries, with bonding to four O atoms and two OH molecules; instead, they may be bonded to five O atoms and only one OH molecule or to six O atoms and no OH molecules. Because the Mössbauer measurements are sensitive primarily to coordination environment and charge density, the Mössbauer spectrum of a H^+-deficient hornblende might theoretically yield doublets corresponding to Fe atoms in up to eight types of polyhedra: M2, M4, M1, and M3 with stoichiometric H^+, M1 and M3 with one H^+, and M1 and M3 with no H^+. Either Fe^{3+} or Fe^{2+} may occupy any of those sites, giving rise (theoretically) to as many as 16 doublets in the spectrum of even a slightly H^+-deficient hornblende. In practice, we were able to resolve no more than seven doublets in any spectrum because of the heavy overlap between peaks; even these fits are questionable because the peak separation is less than that required (½ peak width minimum) for well-resolved peaks (Bancroft, 1973). The assignment of such doublets is complicated further by the fact that the multiplicity of types of environments (as discriminated by the Mössbauer effect) no longer corresponds to the known site multiplicity of M1:M2:M3:M4 equal to 2:2:1:2.

In light of these uncertainties in interpretation of multiple doublet fits, the strategy used in the present study was to fit six peaks initially (a three doublet fit) to each spectrum. We were able to resolve three doublets in every spectrum, as shown in Table 3 and Figure 3. This method resulted in low values of χ^2, percent Misfit, and percent uncertainty for each spectrum and yielded a relatively consistent set of peak parameters, as shown by the small standard deviations in Table 3. The values of percent Fe^{3+} that resulted are thus a valid representation of the total percent of Fe^{3+} contributions to the spectra. It should also be noted that the number of doublets fitted to model Fe^{3+} does not affect the final percent of Fe^{3+} determined. For these spectra, even six doublet fits yielded exactly the

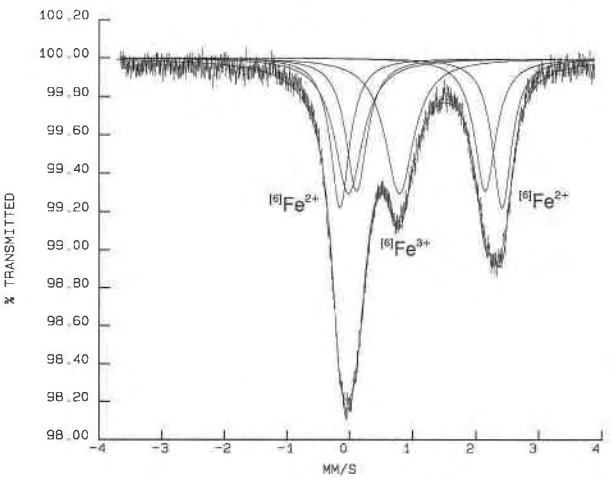

Fig. 3. Mössbauer spectrum of sample Ba-5, fitted with a three doublet model. Two doublets corresponding to $^{[6]}Fe^{2+}$ and one doublet corresponding to $^{[6]}Fe^{3+}$ are shown. A three doublet model was used to fit all spectra in this study; results are given in Table 3 and used in the formula recalculations in Table 4.

same percent of Fe^{3+} total peak area as the three doublet fits; i.e., the percent Fe^{3+} determined by Mössbauer is model-independent for these samples.

However, the three doublet model does not allow accurate interpretation of the location of the Fe atoms in the structure because the area contained in each doublet may represent contributions from Fe in more than one site (because of the similarity between an M1 or M3 site in an anhydrous amphibole and a normal M2 site, as discussed above). This conclusion is supported by the peak widths given in Table 3, which are much larger than the line widths typically observed for Fe in single sites in silicates: 0.27–0.28 mm/s for Fe^{2+} and 0.28–0.35 mm/s for Fe^{3+} (Bancroft, 1973). Only in the case of sample Fr-12 were we able to resolve three unique doublets corresponding to three sites (for Fe^{3+}). We interpret the doublets, which have δ = 0.38, 0.40, and 0.40 mm/s and Δ = 1.56, 1.16, and 0.70 mm/s, to represent Fe^{3+} occupancy in M2, M3, and M1 sites, respectively, as explained earlier. For other samples, four, five, and six doublet models were also fitted to each spectrum as far as possible. However, the heavy peak overlap that results from such fits renders them mathematically possible but crystal-chemically unbelievable.

In order to evaluate the true Fe^{3+} contents of our mantle kaersutite samples, it was necessary to establish a viable value for *C*, the correction factor. Eight samples from a metamorphic suite analyzed by Cosca et al. (1991) were fitted with six peak fits, as shown in the bottom portion of Table 3. Direct comparison of the results is shown in Table 4. An average correction factor, or *C* value, of 1.22 ± 0.06 was obtained. Previous work by Bancroft and Brown (1975) and Bahgat and Fayek (1982), who derived values of 1.13 ± 0.02, and 1.15, respectively, may have been biased by lack of good H analyses for their samples. However, our value of 1.22 agrees well with the two kaersutite *C* values determined by Whipple (1972): 1.25 and 1.24. Therefore, we have applied our correction factor of 1.22 to all the Mössbauer results presented in this paper, and corrected values for percent of Fe^{3+} have been used in Table 5 and in related figures.

TABLE 4. Results of comparative study of amphiboles

Sample	U.U. Wt% H_2O	S.M.U. Wt% H_2O	U.U. %Fe^{3+}	U.O. %Fe^{3+}	*C*
SSA-5	1.68	1.63	29	33	1.210
HL862C	1.88	1.92	35	38	1.135
		2.26			
MR-865A	1.78	1.68	22	25	1.178
		1.62			
MIN 864	1.80	1.73	33	38	1.264
SSA-10	1.75	1.42	23	28	1.314
FA86-1	1.23	1.35	18	21	1.236
HL8611	1.64	*	31	36	1.264
SAS-13	1.41	1.38	35	38	1.143
Average					1.218 ± 0.059

Note: analyses performed at University of Utah (U.U.), Southern Methodist University (S.M.U.), and University of Oregon (U.O.).
* Insufficient sample was available for analysis.

H^+ contents

H analyses were obtained for seven of the eight samples provided from the Cosca et al. (1991) study of metamorphic samples; results are shown in Table 4. The largest difference between the two laboratories is the 0.33 wt% H_2O difference for sample SSA-10. The remaining analyses agree well within the commonly stated error bar of ±0.1 wt% H_2O. The results suggest that there is no substantive difference between the yields obtained using the apparatus at Utah (as used by Cosca et al., 1991) and the line used at S.M.U.

F contents

PIGE analyses of the kaersutite samples showed only minor variations in F contents, ranging from a low of 167 ppm for the San Carlos sample to a high of 3054 ppm for the Eifel specimen. In contrast with conclusions reached by Kyser (1992) on a suite of kaersutite samples, we find that halogen variation alone cannot explain the range of observed H^+ contents in our sample suite.

Chemical formulae

Chemical compositions for all samples and for the average of all samples studied were determined from probe, Mössbauer, PIGE, and H-extraction data and are given in Table 5. The Fe and Fe_2O_3 contents were calculated from the probe data using the corrected Mössbauer measurements from the six peak fits given in Table 3 and the *C* value of 1.22. Data were normalized to formula units with 24 O atoms and adjusted to account for the contributions of F and Cl.

TABLE 5. Hornblende compositions

	DL-5	DL-7	DL-9	AK-M1	AK-M2	AK-M3	AK-M4	AK-M5	Ba-5	Tm	Fr-11	Fr-12	84-BR
SiO_2	38.91	39.85	39.01	39.73	39.93	40.28	40.01	39.20	40.41	39.52	40.05	39.82	39.29
Al_2O_3	14.64	14.39	14.26	14.85	14.83	14.82	15.20	14.11	14.60	14.03	14.48	14.53	13.85
TiO_2	4.84	4.51	4.52	5.21	5.31	5.32	4.98	5.14	4.52	5.87	4.49	4.30	3.27
FeO	7.92	8.17	0.14	8.20	8.27	8.67	8.83	7.95	6.89	2.84	3.58	0.00	5.88
Fe_2O_3	4.43	6.36	13.27	3.53	3.07	3.73	3.97	5.04	4.37	10.40	10.34	13.95	5.15
MgO	12.16	11.26	12.31	12.11	12.84	12.22	12.01	11.68	13.07	11.71	11.92	12.12	13.77
MnO	0.17	0.20	0.15	0.08	0.09	0.13	0.12	0.11	0.14	0.17	0.12	0.14	0.10
CaO	11.02	10.82	10.71	9.98	9.87	9.79	9.39	9.37	10.36	11.10	10.73	10.82	12.10
Na_2O	2.61	2.74	2.61	2.86	2.91	3.30	3.37	3.10	2.66	2.81	2.73	2.77	1.96
K_2O	1.66	1.50	1.64	1.14	1.10	1.24	0.92	1.12	1.55	1.29	1.35	1.38	2.18
Cr_2O_3	0.03	0.00	0.02	0.03	0.02	0.04	0.00	0.00	0.01	0.00	0.02	0.02	0.02
F	0.14	0.17	0.20	0.15	0.17	0.16	0.12	0.13	0.16	0.24	0.16	0.11	0.22
Cl	0.01	0.02	0.02	0.00	0.00	0.00	0.00	0.01	0.00	0.00	0.00	0.00	0.00
H_2O	1.05	0.90	0.16	1.01	1.03	0.96	0.92	0.84	1.03	0.07	0.48	0.17	1.32
Total	99.59	100.89	99.02	98.88	99.44	100.66	99.84	97.80	99.77	100.05	100.45	100.13	99.11
Cations to 24 O atoms minus F and Cl atoms													
Si	5.81	5.89	5.85	5.92	5.90	5.92	5.93	5.94	5.95	5.88	5.92	5.96	5.84
Al	2.58	2.51	2.52	2.61	2.58	2.57	2.65	2.52	2.54	2.46	2.52	2.57	2.43
Ti	0.54	0.50	0.51	0.58	0.59	0.59	0.55	0.59	0.50	0.66	0.50	0.48	0.37
Fe^{2+}	0.99	1.03	0.21	1.02	1.02	1.06	1.09	1.02	0.86	0.46	0.54	0.00	0.75
Fe^{3+}	0.49	0.69	1.31	0.40	0.34	0.41	0.44	0.57	0.48	1.06	1.06	1.37	0.56
Mg	2.71	2.48	2.75	2.69	2.83	2.68	2.65	2.64	2.87	2.60	2.63	2.71	3.05
Mn	0.02	0.03	0.02	0.01	0.01	0.02	0.02	0.01	0.02	0.02	0.02	0.02	0.01
Ca	1.76	1.71	1.72	1.59	1.56	1.54	1.49	1.52	1.64	1.77	1.70	1.74	1.93
Na	0.76	0.79	0.76	0.83	0.83	0.94	0.97	0.91	0.76	0.81	0.78	0.80	0.57
K	0.32	0.28	0.31	0.22	0.21	0.23	0.17	0.22	0.29	0.24	0.25	0.26	0.41
Cr	0.00	0.00	0.00	0.00	0.00	0.00	0.00	0.06	0.00	0.00	0.00	0.00	0.00
F	0.07	0.08	0.09	0.07	0.08	0.07	0.06	0.06	0.08	0.11	0.08	0.05	0.10
Cl	0.00	0.01	0.01	0.00	0.00	0.00	0.00	0.00	0.00	0.00	0.00	0.00	0.00
H	1.05	0.89	0.16	1.00	1.02	0.94	0.91	0.85	1.01	0.06	0.47	0.17	1.31

DISCUSSION

Measured vs. calculated Fe^{3+} and H^+

Calculations of amphibole Fe^{3+} contents based on various charge balance arguments abound in the literature (e.g., Stout, 1972; Papike et al., 1974). Schumacher (1991) discussed the effects of such empirical corrections on amphibole geothermometry, and Hawthorne (1983) thoroughly covered the many reasons why there is "(unfortunately) no significant correlation" between Fe^{3+} values thus calculated and those that have been measured. This conclusion is also true for our data, as shown in Figure 4a, where Fe^{3+} is calculated solely on the basis of charge balance.

Clowe et al. (1988) described a method for calculating the oxyamphibole content of amphibole for which both electron microprobe and Fe^{3+}/Fe_{tot} data are available (in their case, the Fe^{3+}/Fe_{tot} values were determined by calorimetry). The process involves correction of an analysis based on 23 O atoms by recalculating the probe-determined total elemental wt% Fe to elemental Fe^{3+} and Fe^{2+}, followed by conversion to weight percent oxide and moles of Fe^{3+} and Fe^{2+}, and renormalization to 23 O atoms + $\frac{1}{2}Fe^{3+}$ pfu. They note that this method makes the assumption that Fe^{3+} is present as an oxyamphibole component, with one Fe^{3+} for every H^+ lost.

Their method was tested on the samples in the present data set using the Fe^{3+}/Fe_{tot} values determined by Mössbauer and corrected for recoil-free fraction; the results are shown in Figure 4b. Although this figure shows some general agreement between the H^+ calculated in this way and the measured H^+, the calculated values are consistently too high. In addition to the problems associated with assumptions of perfect stoichiometry and charge balance discussed by Hawthorne (1983), such a recalculation scheme is also strongly biased by its dependence on measured Si content, an element that is particularly difficult to measure accurately by microprobe. Note also that this recalculation depends on accurate assessment of Fe^{3+} contents.

Mechanisms for Fe^{3+} substitution

As discussed above, Popp et al. (1990) have identified three likely mechanisms for the accommodation of Fe^{3+} in the amphibole structure, which can be expressed as the following substitution vectors: (1) $Fe^{2+}H^+Fe^{3+}_{-1}$, oxysubstitution (or deprotonation) with H^+ providing charge balance for the Fe^{2+}, (2) $^{[6]}Al^{3+}Fe^{3+}_{-1}$, substitution of Al^{3+} for Fe^{3+}, (3) $^{[A]}(K,Na)Fe^{2+}{}_{-[A]}\square_{-1}Fe^{3+}_{-1}$, replacement of an Fe^{3+} and a vacant A site by a Fe^{2+} and either a K or Na in the A site. Each of these relationships is plotted in Figure 5. It is immediately obvious from the nearly 1:1 inverse correlation between H^+ and Fe^{3+} that the bulk of the Fe^{3+} variation can be explained by the relationship representing the oxysubstitution mechanism 1. A linear regression fit to the plot of H^+ vs. Fe^{3+} yields a slope of -0.80 ± 0.10, with a correlation coefficient of 0.88. The deviations from a 1:1 inverse relationship (slope of -1) are probably indicative of other less important substitutions and of the limitations of the electron microprobe

TABLE 5.—*Continued*

86-BM	86-LEH	H366A	H366-92	S.C.	K.N.Z.	Eifel
41.91	41.52	39.76	39.61	40.87	39.32	38.00
14.46	15.05	14.04	14.77	14.76	13.54	13.69
3.23	2.50	4.34	5.19	3.29	4.89	4.37
6.11	7.51	9.97	0.72	7.50	7.85	8.09
2.06	3.07	3.37	12.34	4.01	3.53	6.30
15.16	14.70	11.29	12.41	12.90	12.31	11.43
0.11	0.10	0.15	0.12	0.17	0.14	0.31
10.74	10.17	10.24	10.43	10.94	9.96	10.27
3.18	2.88	2.90	2.82	2.97	2.56	2.18
1.21	0.96	1.52	1.44	1.05	2.06	2.37
0.77	0.12	0.00	0.00	0.00	0.00	0.00
0.08	0.07	0.15	0.16	0.02	0.18	0.31
0.00	0.00	0.00	0.00	0.01	0.02	0.07
1.13	1.23	1.18	0.13	0.69	1.14	1.18
100.15	99.88	98.91	100.14	99.18	97.50	98.57
Cations to 24 O atoms minus F and Cl atoms						
6.10	6.07	5.98	5.85	6.10	5.95	5.74
2.48	2.59	2.49	2.57	2.60	2.42	2.44
0.35	0.27	0.49	0.58	0.37	0.56	0.50
0.74	0.92	1.25	0.09	0.94	0.99	1.04
0.23	0.34	0.39	1.37	0.45	0.40	0.70
3.29	3.20	2.53	2.73	2.87	2.78	2.57
0.01	0.01	0.02	0.02	0.02	0.02	0.04
1.67	1.59	1.65	1.75	1.62	1.66	1.68
0.90	0.82	0.85	0.81	0.86	0.75	0.64
0.22	0.18	0.29	0.27	0.20	0.40	0.46
0.09	0.01	0.00	0.00	0.00	0.00	0.00
0.04	0.03	0.07	0.07	0.01	0.09	0.15
0.00	0.00	0.00	0.00	0.00	0.01	0.02
1.10	1.20	1.18	0.13	0.69	1.15	1.19

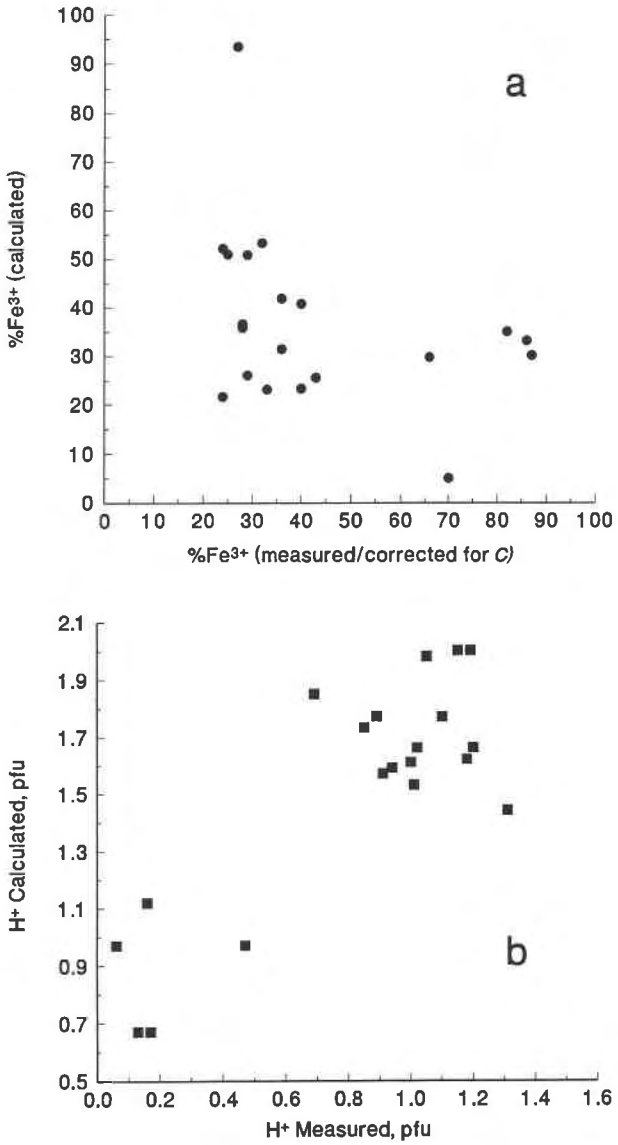

Fig. 4. Calculated vs. measured Fe^{3+} (**a**) and H^+ (**b**) contents of amphiboles. Calculations follow the procedure described in Clowe et al. (1988). Measured and corrected Fe^{3+} data points are Mössbauer data corrected for $C = 1.22$.

and wet chemical techniques in performing such sensitive measurements.

Examination of Figure 5 yields two further observations relating to H^+ contents. At one extreme, where Fe^{3+} reaches its theoretical minimum of zero, H^+ contents do not equal the stoichiometric 2 H^+ pfu; instead, the intercept is 1.32 ± 0.18. This observation underscores the idea that bulk composition, particularly substitution of tetravalent ions such as Ti^{4+} on trivalent sites and trivalent ions on divalent sites, probably controls the amount of H^+ that can be contained in the amphibole structure at mantle pressures and temperatures. At the other extreme, the intercept at the hypothetical zero H^+ is very close to three data points representing almost H^+-free amphibole. Thus, true oxykaersutite probably exists and is certainly stable at surface pressures and temperatures.

Implications for mantle metasomatism

As indicated above, the H^+/Fe^{3+} data plotted in Figure 5 display a near 1:1 inverse relationship between the H^+ and Fe^{3+} contents in the kaersutite samples. The data fall into two clusters: the first, Fe^{3+} contents of about 0.4 pfu and H^+ contents of about 1.1 pfu, generally show <25% dehydrogenation; the second, with much higher Fe^{3+} (near 1.3 pfu) and lower H^+ (near 0.1 pfu), show about 90% hydrogenation. There are four possible interpretations of these data: (1) the amphibole samples were partially dehydrogenated during ascent from the upper mantle; (2) dehydrogenation occurred after the amphibole samples were erupted onto the Earth's surface; (3) the amphibole samples were dehydrogenated during a metasomatic event in the upper mantle subsequent to amphibole growth but prior to entrainment and transport; or (4) the amphibole samples crystallized in regions of the upper mantle that were chemically distinct (in terms of O and/or H activity). Each of these interpretations will be discussed below in light of petrographic observations of the megacrysts and their host rocks, as well as experimental constraints on dehydrogenation of the hornblende.

Kinetics of dehydrogenation

The correlation between H^+ and Fe^{3+} in these hornblende samples may be compared with observations from

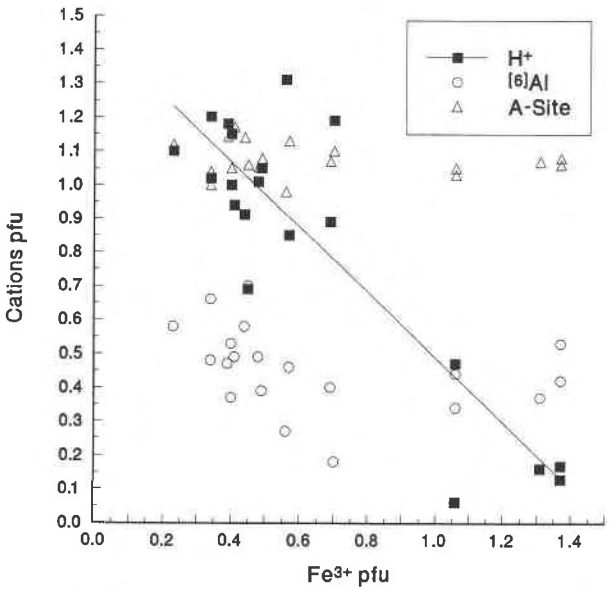

Fig. 5. Fe^{3+} substitution mechanisms for amphiboles, as suggested by Popp et al. (1990).

experiments investigating the hydrogenation of olivine crystals at temperatures from 800 to 1000 °C. From their results, Mackwell and Kohlstedt (1990) concluded that H was incorporated as protons in the crystal structure of olivine through a reaction involving the consumption of polarons (the excess charge on the Fe^{3+}):

$$\tfrac{1}{2}[H_2]_{gas} + Fe^{3+}_{ol} \rightleftharpoons H^+_{ol} + Fe^{2+}_{ol}$$

resulting in a predicted 1:1 inverse correlation between H^+ and Fe^{3+}. At higher temperatures (1300 °C), Bai and Kohlstedt (1992) have shown that defect relaxation on the major element sublattices permits a decoupling of the H^+ and Fe^{3+}. A similar process might be expected to occur in reverse in hornblende, with dehydrogenation resulting in a parallel increase in Fe^{3+} at moderate temperatures (Dyar et al., 1992b).

Graham et al. (1984) have measured H diffusivities in hornblende experimentally from isotope exchange measurements at temperatures in the range 350–850 °C. We have replotted the data of Graham et al. (1984) for pargasitic hornblende 322 and ferroan pargasitic hornblende 6099 in Figure 6. We see no reason why there should be significant differences in diffusivities for hornblende samples of such similar compositions and therefore have generated linear regression fits to their data for both hornblende samples assuming plate and cylinder geometries. Also plotted on the figure is a data point calculated from the infrared observations of Skogby and Rossman (1989) for the sample that they dehydrated at room pressure and 700 °C in air. This result is in good agreement with those of Graham et al. (1984).

As the major element compositions of the hornblende samples investigated in this study are quite similar to those of Graham et al. (1984), we extrapolated their results to higher temperatures to determine the times necessary for partial or total dehydrogenation of the kaersutite crystals. Although they determined their diffusivities from isotope exchange experiments, as opposed to dehydrogenation experiments, the general agreement of their data with the results from the experiments of Skogby and Rossman (1989) suggests that the kinetics of the two processes are similar. We modeled the dehydrogenation process assuming the reaction given above for olivine and using a simple calculation of the diffusivity for H necessary to produce partial dehydrogenation of hornblende crystals of a particular grain size. In this calculation, we assumed that diffusion is essentially one-dimensional and obeys a relationship determined for diffusion in a finite slab with an infinite sink for H at the grain edges (see e.g., Schmalzried, 1981; p. 85). It is assumed in this calculation that dehydrogenation is driven by the partitioning of H/H_2O from the crystalline hornblende into the surrounding melt phase, and that the rate of defect reequilibration on the major ion sublattices in the crystals is slow. Although no data exist for reequilibration of point defects in amphibole, Mackwell et al. (1988) have shown that, for olivine crystals at 1200 °C, defect reequilibration on the octahedral cation sublattice takes on the order of 10 d for crystals with a grain size of about 10 mm.

Dehydrogenation of kaersutite?

The kaersutite samples investigated in this study were generally crystals on the order of 10 mm, although this figure should probably be taken as an underestimate, as most of the crystals showed evidence of surface breakdown during transport. The partial breakdown of the hornblende also provides some constraints on the temperatures (probably 1100–1250 °C) and time scales (probably between several hours and a month) of entrainment and ascent (e.g., Spera, 1984). In Figure 6, the horizontal extent of the boxes in the upper left indicates this temperature range, while the vertical extent of each box indicates the time span from 3 h (bottom) to 30 d (top) for 10 mm of hornblende to reach 10, 25, or 90% dehydrogenation. Although the cluster of H^+-Fe^{3+} data with lesser degrees (<25%) of dehydrogenation (upper left, Fig. 5) might be explained by partial dehydrogenation during ascent, the data that show almost total dehydrogenation (lower right, Fig. 5) would require diffusivities that are far in excess of those predicted by the results of Graham et al. (1984). This latter observation may be interpreted as indicating that the Graham et al. (1984) data are not valid at the higher temperatures of the hornblende source region. However, it seems unlikely that the diffusivity would change by 3–4 orders of magnitude over the range from 850 °C in the experiments to 1000–1200 °C in the Earth, particularly given the similar chemical compositions of the two suites of hornblende specimens.

The right axis for Figure 6 shows the amount of time necessary for 90% dehydrogenation of a hornblende with a 10 mm grain size. If we extrapolate the data of Graham et al. (1984) to 1200 °C, the time required for significant loss of H (90%) from the kaersutite samples is on the order of 3–30 yr. Thus, despite our earlier speculation

(Dyar et al., 1992b), it seems unlikely that the entire ranges of H^+ and Fe^{3+} observed in this hornblende suite can be explained by dehydrogenation during transport, as only limited H loss is possible by this mechanism.

The second possible explanation for the observed range in H^+/Fe^{3+} would be that the kaersutite samples maintained a sufficiently high temperature over a protracted period subsequent to emplacement on the Earth's surface, during which time dehydrogenation could occur. Although this possibility may be plausible for megacrysts entrained in a thick sequence of lava deposits or emplaced adjacent to a long-lived lava lake, it is unable to account for the low H^+ observed in samples that show evidence of eruption as ejecta.

The third possibility, that of a long-term interaction with a mantle fluid after crystallization but prior to entrainment is also unsupported by petrographic analysis. For a silicate melt to produce nearly total dehydrogenation of kaersutite would require an interaction over a period of years that should leave clear petrographic evidence and zoning in the major element compositions. Such evidence has been looked for but is not observed.

The final explanation requires distinct chemical differences in the metasomatic fluids from which the various hornblende samples crystallized in the subcontinental mantle, in accord with the recent observations of Ionov and Wood (1992), and Amundsen and Neumann (1992). Thus, for the hornblende samples in the lower right in Figure 5, the high Fe^{3+} contents might reflect relatively more oxidizing conditions in the metasomatic fluid, with the low H^+ contents occurring because H incorporation would not be required for charge balance during growth: the hornblende would grow as oxykaersutite. The suite of hornblende samples in the upper left of Figure 5 could then be explained as normal kaersutite specimens, some of which partially dehydrogenated during entrainment and ascent. Although both types of kaersutite may be found in the same geographic locality (e.g., the Saudi and Deadman Lake samples), the entraining basaltic melt traversed large regions of the upper mantle during its ascent to the surface and may have sampled hornblende megacrysts from a number of quite distinct chemical reservoirs. Such a model requires either that the metasomatic fluids varied chemically over time within the region sampled by the basalt, or that local heterogeneities in the chemical signature of the metasomatic fluids occur over a spatial scale of a few tens of kilometers or less.

The experimental data clearly indicate that significant dehydration of the hornblende is unlikely on the time scales of mobilization and transport of hornblende megacrysts with crystal sizes near 10 mm. Thus, we concur with Graham et al. (1984) that "amphibole crystals in rapidly quenched lavas will, in the absence of extensive oxidation of alteration, preserve their high-temperature (magmatic) H isotope composition, and they should therefore preserve useful information on the H isotope compositions and origins of 'magmatic' waters." Consequently, we would argue that, at least for the kaersutite samples investigated in this study, high Fe^{3+} contents are probably indicative of chemical heterogeneity of the mantle source regions.

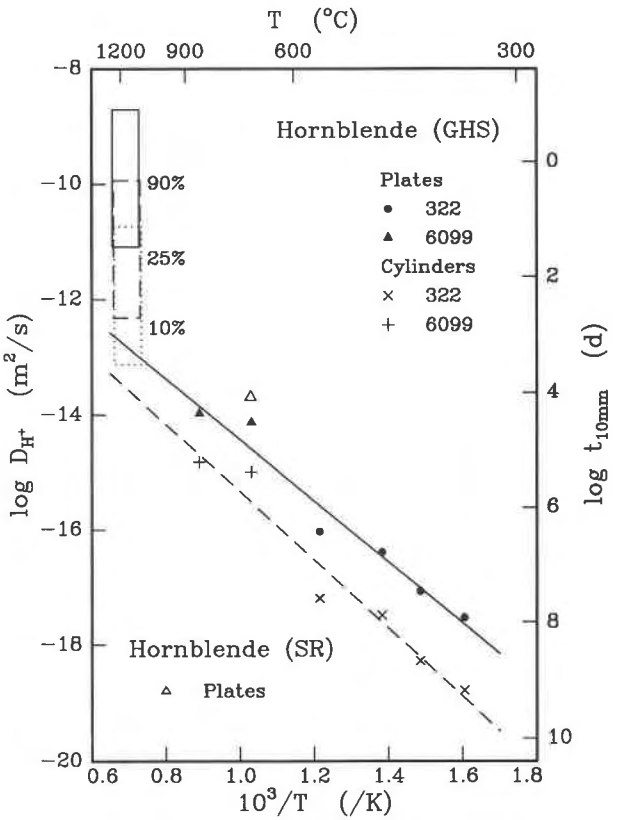

Fig. 6. A plot of H diffusivity vs. temperature for pargasitic hornblende using the data of Graham et al. (1984) (GHS) and a value inferred from the observations of Skogby and Rossman (1989) (SR). The boxes in the upper left of the figure show the diffusivities necessary to produce the percentage indicated of H loss for 10-mm hornblendes over the temperature range from 1100 to 1250 °C on a time scale of 3 h to 30 d.

Conclusions

1. Mössbauer spectra measured on a suite of 20 mantle kaersutite samples reveal a range of Fe^{3+} contents from 100% Fe^{3+} to only 21% Fe^{3+}. Spectra can be interpreted with simple three doublet models. More complicated fits are mathematically possible but lack physical relevance because heavy overlap between peaks renders the resultant fits nonunique.

2. Comparison with wet chemical results of Fe^{3+}/Fe^{2+} determinations on a suite of metamorphic amphibole samples permits calculation of an improved value of $C = 1.22$ for the recoil-free fraction correction factor in kaersutite.

3. H^+ contents as determined by U extraction techniques range from 0.07 to 1.32 wt% H_2O. Careful determination of F by PIGE spectroscopy and Cl by electron microprobe shows that these elements are present in only minor amounts; thus, H^+ variation cannot be explained by halogen contents.

4. H^+ contents of the kaersutite samples vary in a nearly 1:1 inverse relationship with Fe^{3+} contents. Although the range of Fe^{3+}/H^+ in the less oxidized kaersutite megacrysts may be explained by partial H loss during entrainment and ascent, the near total dehydrogenation of the Fe^{3+}-rich megacrysts would require time scales significantly longer than is expected for transport. Thus, it seems likely that these oxykaersutite samples grew in a more oxidized metasomatic fluid, where incorporation of H was not required for charge compensation. As megacrysts from the same location show wide variation in Fe^{3+} and H^+, it appears likely that significant variations in the oxidation state of the mantle metasomatic fluid occurred over relatively small temporal or spatial scales.

Acknowledgments

Supported by National Science Foundation grants EAR-90-17167 (A.V.M.), EAR-93-05187 (S.J.M.), and EAR-93-04304 (M.D.D.). We thank Howard Wilshire for the loan of samples from his personal collection, Michael Cosca for use of samples from Cosca et al. (1991), and the staff at the National Museum of Natural History for assistance in obtaining samples from the Coleman collection. We also acknowledge Kipp Bajaj, Tim Day, Mike Harrell, Marjorie Taylor, and Heather Wilcox for assistance with sample preparation, and M.T. Colucci, R. Gregory, and C.B. Douthitt for logistical support of the isotope data. We are grateful for thoughtful reviews by Roger Burns, Michael Cosca, Etienne Deloule, Colin Graham, and Claude Herzberg. Mössbauer and H^+ analyses were funded by the Mineral Spectroscopy Laboratory at the University of Oregon.

References cited

Aldridge, L.P., Tse, J.S., and Bancroft, G.M. (1982) The identification of Fe^{2+} in the M4 site of calcic amphiboles: Discussion. American Mineralogist, 67, 335–339.

Amundsen, H.E.F., and Neumann, E.-R. (1992) Redox control during mantle/melt interaction. Geochimica et Cosmochimica Acta, 56, 2405–2416.

Andersen, T., O'Reilly, S.Y., and Griffin, W.L. (1984) The trapped fluid phase in upper mantle xenoliths from Victoria, Australia: Implications from mantle metasomatism. Contributions to Mineralogy and Petrology, 88, 72–85.

Aoki, K.-I. (1963) The kaersutites and oxykaersutites from alkalic rocks of Japan and surrounding areas. Journal of Petrology, 4, 198–210.

——— (1970) Petrology of kaersutite-bearing ultramafic and mafic inclusions in Iki Island, Japan. Contributions to Mineralogy and Petrology, 25, 270–283.

——— (1971) Petrology of mafic inclusions from Itinome-gata, Japan. Contributions to Mineralogy and Petrology, 30, 314–331.

Bahgat, A.A., and Fayek, M.K. (1982) Absolute evaluation of ferrous and ferric concentration in Ca amphibole. Physica Status Solidi A, 71, 575–581.

Bai, Q., and Kohlstedt, D.L. (1992) Substantial hydrogen solubility in olivine and implications from water storage in the mantle. Nature, 357, 672–674.

Bailey, D.K. (1970) Volatile flux, heat focusing, and generation of magma. Geological Journal Special Issue, 2, 177–186.

——— (1972) Uplift rifting and magmatism in continental plates. Leeds Journal of Earth Sciences, 8, 225–239.

Bancroft, G.M. (1973) Mössbauer spectroscopy: An introduction for inorganic chemists and geochemists, p. 34. McGraw-Hill, New York.

Bancroft, G.M., and Brown, J.R. (1975) A Mössbauer study of coexisting hornblendes and biotites: Quantitative Fe^{3+}/Fe^{2+} ratios. American Mineralogist, 60, 265–272.

Barnes, V.E. (1930) Changes in hornblende at about 800°C. American Mineralogist, 15, 393–417.

Bergman, S.C. (1981) Fluid inclusions in xenoliths: Samples of the mantle metasomatic fluid? Geological Society of America Abstracts with Programs, 13, 408.

Best, M.G. (1970) Kaersutite-peridotite inclusions and kindred megacrysts in basanitic lavas, Grand Canyon, Arizona. Contributions to Mineralogy and Petrology, 27, 25–44.

——— (1974) Mantle-derived amphibole within inclusions in alkalic-basaltic lavas. Journal of Geophysical Research, 79 (14), 2107–2113.

Bigeleisen, J., Perlman, M.L., and Prosser, H.C. (1952) Conversion of hydrogenic materials to hydrogen for isotopic analysis. Analytical Chemistry, 24, 1356–1357.

Boettcher, A.L., and O'Neil, J.R. (1980) Stable isotope, chemical, and petrographic studies of high pressure amphiboles and micas: Evidence for metasomatism in the mantle source regions of alkali basalts and kimberlites. American Journal of Science, 280-A, 594–621.

Bryndzia, L.T., Davis, A.M., and Wood, B.J. (1990) The isotopic composition (δD) of water in amphiboles and the redox state of amphibole-bearing upper mantle spinel peridotites. Geological Society of America Abstracts with Programs, 22 (7), A254.

Burns, R.G., and Greaves, C.J. (1971) Correlations of infrared and Mössbauer site populations of actinolites. American Mineralogist, 56, 2010–2033.

Burns, R.G., Greaves, C.J., Law, A.D., Tew, M.J., and Prentice, F.J. (1970) Assessment of the reliability of the Mössbauer and infrared methods in site-population studies of amphiboles. Geological Society of America Abstracts with Programs, 2, 509–511.

Burns, R.G., Burns, V.M., Dyar, M.D., Ryan, V.L., and Solberg, T. (1985) Iron coordination symmetries in silicates: Correlations from Mössbauer parameters of Fe^{2+} and Fe^{3+}. Geological Society of America Abstracts with Programs, 17 (7), 535.

Canil, D., Virgo, D., and Scarfe, C.M. (1990) Oxidation state of mantle xenoliths from British Columbia, Canada. Contributions to Mineralogy and Petrology, 104, 453–462.

Clowe, C.A., Popp, R.K., and Fritz, S.J. (1988) Experimental investigation of the effect of oxygen fugacity on ferric-ferrous ratios and unit cell parameters of four natural clinoamphiboles. American Mineralogist, 73, 487–499.

Cosca, M.A., Essene, E.J., and Bowman, J.R. (1991) Complete chemical analyses of metamorphic hornblendes: Implications for normalizations, calculated H_2O activities, and thermobarometry. Contributions to Mineralogy and Petrology, 108, 472–484.

Deloule, E., Albarède, F., and Sheppard, S.M.F. (1990) *D/H* analysis of amphiboles from mantle lherzolite xenoliths by ion probe. International Conference on Geochronology, Cosmochronology, and Isotope Geology, 7, 26.

——— (1991) Hydrogen isotope heterogeneities in the mantle from ion probe analysis of amphiboles from ultramafic rocks. Earth and Planetary Science Letters, 105, 543–553.

Dick, H.J.B., Fisher, R.L., and Bryan, W.B. (1984) Mineralogic variability of the uppermost mantle along mid-ocean ridges. Earth and Planetary Science Letters, 69, 88–106.

Dodge, F.C.W., Papike, J.J., and Mays, R.E. (1968) Hornblendes from granite rocks of the Central Sierra Nevada Batholith, California. Journal of Petrology, 9, 378–410.

Dyar, M.D. (1984) Precision and interlaboratory reproducibility of measurements of the Mössbauer effect in minerals. American Mineralogist, 69, 1127–1144.

Dyar, M.D., McGuire, A.V., and Ziegler, R.D. (1989) Redox equilibria and crystal chemistry of coexisting minerals from spinel lherzolite mantle xenoliths. American Mineralogist, 74, 969–980.

Dyar, M.D., McGuire, A.V., and Harrell, M.D. (1992a) Redox behavior in contrasting styles of metasomatism in the upper mantle. Geochimica et Cosmochimica Acta, 56, 2579–2586.

Dyar, M.D., McGuire, A.V., and Mackwell, S.J. (1992b) Fe^{3+}/H^+ and *D/H* in kaersutites: Misleading indicators of mantle source fugacities. Geology, 20, 565–568.

Ernst, W.G., and Wai, C.M. (1970) Mössbauer, infrared, X-ray, and optical study of cation ordering and dehydrogenation in natural and heat-treated sodic amphiboles. American Mineralogist, 55, 1226–1258.

Goldman, D.S., and Rossman, G.R. (1977) The identification of Fe^{2+} in the M(4) site of calcic amphiboles. American Mineralogist, 62, 205–216.

Goodman, B.A., and Wilson, M.J. (1976) A Mössbauer study of the weathering of hornblende. Clay Minerals, 2, 153–163.

Graham, C.M., Harmon, R.M., and Sheppard, S.M.F. (1984) Experimental hydrogen isotope studies: Hydrogen isotope exchange between amphibole and water. American Mineralogist, 69, 128–138.

Harte, B., Cox, K.G., And Gurney, J.J. (1975) Petrography and geological history of upper mantle xenoliths from Matsoku Kimberlite pipe. Physics and Chemistry of the Earth, 9, 477–506.

Hawthorne, F.C. (1978) The crystal chemistry of the amphiboles. VI. The stereochemistry of the octahedral strip. Canadian Mineralogist, 16, 37–52.

——— (1981) Crystal chemistry of the amphiboles. In Mineralogical Society of America Reviews in Mineralogy, 9A, 1–102.

——— (1983) The crystal chemistry of the amphiboles. Canadian Mineralogist, 21, 173–480.

Hawthorne, F.C., and Grundy, H.D. (1973) The crystal chemistry of the amphiboles. II. Refinement of the crystal structure of oxy-kaersutite. Mineralogical Magazine, 39, 390–400.

Holdaway, M.J., Dutrow, B.L., Borthwick, J., Shore, P., Harmon, R.S., and Hinton, R.W. (1986) H content of staurolite as determined by H extraction line and ion microprobe. American Mineralogist, 71, 1135–1141.

Ionov, D.A., and Wood, B.J. (1992) The oxidation state of subcontinental mantle: Oxygen thermobarometry of mantle xenoliths from central Asia. Contributions to Mineralogy and Petrology, 111, 179–193.

Jirák, Z., Pechar, F., and Vratislov, S. (1986) Distribution of cations and the proton location in kaersutite. Crystallographic Research and Technology, 21, 1517–1519.

Kitamura, M., and Tokonami, M. (1971) The crystal structure of kaersutite. Scientific Reports of the Tohoku University, Series 3, 11, 125–141.

Kuroda, Y., Hariya, Y., Suzuoki, T., and Matsuo, S. (1978) Hydrogen isotope study on biotite and hornblende from Finnish granitic rocks. Geochemical Journal, 12, 259–263.

Kyser, T.K. (1992) Hydrogen isotope systematics of mafic magmas and mantle minerals (abs.). Eos, 73, 348.

Mackwell, S.J., and Kohlstedt, D.L. (1990) Diffusion of hydrogen in olivine: Implications for water in the mantle. Journal of Geophysical Research, 95, 5079–5088.

Mackwell, S.J., Dimos, D., and Kohlstedt, D.L. (1988) Transient creep of olivine: Point defect relaxation times. Philosophical Magazine, 57, 779–789.

Matson, D.W., Muenow, D.W., and Garcia, M.O. (1984) Volatiles in amphiboles from xenoliths, Vulcan's Throne, Grand Canyon, Arizona. Geochimica et Cosmochimica Acta, 48, 1629–1636.

McGuire, A.V., Dyar, M.D., and Ward, K.W. (1989) Neglected Fe^{3+}/Fe^{2+} ratios: A study of Fe^{3+} content of megacrysts from alkali basalts. Geology, 17, 687–690.

McGuire, A.V., Dyar, M.D., and Nielson, J.E. (1991) Metasomatic oxidation of upper mantle peridotite. Contributions to Mineralogy and Petrology, 107, 252–264.

Menzies, M.A. (1983) Mantle ultramafic xenoliths in alkaline magmas: Evidence for mantle heterogeneity modified by magmatic activity. In C.J. Hawkesworth, and M.J. Norry, Eds., Continental basalts and mantle xenoliths, p. 92–110. Shiva, Nantwich, U.K.

Nielson, J.E., Budahn, J.R., Unruh, D.M., and Wilshire, H.G. (1993) Actualistic models of mantle metasomatism documented in a composite xenolith from Dish Hill, California. Geochimica et Cosmochimica Acta, 57, 105–121.

Oxburgh, E.R. (1964) Petrologic evidence for the presence of amphibole in the upper mantle and its petrogenetic and geophysical implications. Geological Magazine, 101, 1–19.

Papike, J.J., and Clark, J.R. (1968) The crystal structure and cation distribution of glaucophane. American Mineralogist, 53, 1156–1173.

Papike, J.J., Ross, M., and Clarke, J.R. (1969) Crystal-chemical characterization of clinoamphiboles based on five new structure refinements. Mineralogical Society of America Special Paper, 2, 1156–1173.

Papike, J.J., Cameron, K.L., and Baldwin, K. (1974) Amphiboles and pyroxenes: Characterization of OTHER quadrilateral components and estimates of ferric iron from microprobe data. Geological Society of America Abstracts with Programs, 6, 1053–1054.

Pechar, F., Fuess, H., and Joswig, W. (1989) Refinement of the crystal structure of kaersutite (Vlčítbra, Bohemia) from neutron diffraction. Neues Jahrbuch für Mineralogie Monatshefte, 89 (3), 137–143.

Phillips, M.W., Popp, R.K., and Clowe, C.A. (1988) Structural adjustments accompanying oxidation-dehydrogenations in amphiboles. American Mineralogist, 73, 500–506.

Phillips, M.W., Draheim, J.A., Popp, R.K., Clowe, C.A., and Pinkerton, A.A. (1989) Effects of oxidation-dehydrogenation in tschermakitic hornblende. American Mineralogist, 74, 764–773.

Popp, R.K., Phillips, M.W., and Harrell, J.A. (1990) Accommodation of Fe^{3+} in natural Fe^{3+}-rich calcic and subcalcic amphiboles: Evidence from published chemical analyses. American Mineralogist, 75, 163–169.

Roden, M.F., Frey, F.A., and Francis, D.M. (1984) An example of consequent mantle metasomatism in peridotite inclusions from Nunivak Island, Alaska. Journal of Petrology, 25, 546–577.

Roedder, E. (1965) Liquid CO_2 inclusions in olivine-bearing nodules and phenocrysts from basalts. American Mineralogist, 50, 1746–1782.

Ruby, S.L. (1973) Why Misfit when you already have χ^2? In I.J. Gruverman and C.W. Seidel, Eds., Mössbauer effect methodology, p. 263–276. Plenum, New York.

Schmalzried, H. (1981) Solid state reactions, 254 p. Verlag Chemie, Weinheim, Germany.

Schumacher, J.C. (1991) Empirical ferric iron corrections: Necessity, assumptions, and effects on selected geothermobarometers. Mineralogical Magazine, 55, 3–18.

Schwartz, K.B., and Irving, A.J. (1978) Cation valence determinations in kaersutite and biotite megacrysts from alkalic basalts: Evidence for Ti^{4+} in the upper mantle. Eos, 59, 1214–1215.

Sheppard, S.M.F., and Epstein, S. (1970) D/H and $^{18}O/^{16}O$ ratios of minerals of possible mantle or lower crustal origin. Earth and Planetary Science Letters, 9, 232–239.

Skogby, H., and Rossman, G.R. (1989) OH^- in pyroxene: An experimental study of incorporation mechanisms and stability. American Mineralogist, 74, 1059–1069.

Spera, F.J. (1984) Carbon dioxide in petrogenesis. III. Role of volatiles in the ascent of alkaline magmas with special reference to xenolith-bearing mafic lavas. Contributions to Mineralogy and Petrology, 88, 217–232.

Stosch, H.-G., and Seck, H.A. (1980) Geochemistry and mineralogy of two spinel peridotite suites from Dreiser Weiher, West Germany. Geochimica et Cosmochimica Acta, 44, 457–470.

Stout, J.H. (1972) Phase petrology and mineral chemistry of coexisting amphiboles from Telemark, Norway. Journal of Petrology, 13, 99–145.

Varne, R. (1970) Hornblende lherzolite and the upper mantle. Contributions to Mineralogy and Petrology, 27, 45–51.

Whipple, E.R. (1972) Quantitative Mössbauer spectra and chemistry of iron, 205 p. Ph.D. thesis, Massachusetts Institute of Technology, Cambridge, Massachusetts.

Wilshire, H.G. (1987) A model of mantle metasomatism. Geological Society of America Special Paper, 215, 47–60.

Wilshire, H.G., And Shervais, J.W. (1975) Al-augite and Cr-diopside ultramafic xenoliths in basaltic rocks from western United States: Structural textural relationships. Physics and Chemistry of the Earth, 9, 257–272.

Wilshire, H.G., and Trask, N.J. (1971) Structural and textural relationships of amphibole and phlogopite in peridotite inclusions, Dish Hill, California. American Mineralogist, 56, 240–253.

Winchell, A.N. (1945) Variation in composition and properties of calciferous amphiboles. American Mineralogist, 30, 27–50.

Wong, A.S., Robertson, J.D., and Francis, H.A. (1992) Determination of fluorine in coal and coal fly ash by proton-induced gamma-ray emission analysis. Journal of Trace and Microprobe Techniques, 10, 169–181.

Wood, B.J., and Virgo, D. (1989) Upper mantle oxidation state: Ferric iron contents of lherzolite spinels by ^{57}Fe Mössbauer spectroscopy and resultant oxygen fugacities. Geochimica et Cosmochimica Acta, 53, 1277–1291.

Manuscript received October 21, 1992
Manuscript accepted May 13, 1993